Ann. Geophys., 32, 1407–1413, 2014
www.ann-geophys.net/32/1407/2014/
doi:10.5194/angeo-32-1407-2014

Annales Geophysicae
Open Access

Nonlocal nonlinear coupling of kinetic sound waves

O. Lyubchyk[1] **and Y. Voitenko**[2]

[1]Main Astronomical Observatory, National Academy of Sciences of Ukraine, 27 Akademika Zabolotnoho St., 03680 Kyiv, Ukraine
[2]Solar-Terrestrial Centre of Excellence, Belgian Institute for Space Aeronomy, Ringlaan 3 Avenue Circulaire, 1180 Brussels, Belgium

Correspondence to: O. Lyubchyk (olena@mao.kiev.ua)

Received: 22 July 2014 – Revised: 25 September 2014 – Accepted: 6 October 2014 – Published: 13 November 2014

Abstract. We study three-wave resonant interactions among kinetic-scale oblique sound waves in the low-frequency range below the ion cyclotron frequency. The nonlinear eigenmode equation is derived in the framework of a two-fluid plasma model. Because of dispersive modifications at small wavelengths perpendicular to the background magnetic field, these waves become a decay-type mode. We found two decay channels, one into co-propagating product waves (forward decay), and another into counter-propagating product waves (reverse decay). All wavenumbers in the forward decay are similar and hence this decay is local in wavenumber space. On the contrary, the reverse decay generates waves with wavenumbers that are much larger than in the original pump waves and is therefore intrinsically nonlocal. In general, the reverse decay is significantly faster than the forward one, suggesting a nonlocal spectral transport induced by oblique sound waves. Even with low-amplitude sound waves the nonlinear interaction rate is larger than the collisionless dissipation rate. Possible applications regarding acoustic waves observed in the solar corona, solar wind, and topside ionosphere are briefly discussed.

Keywords. Space plasma physics (wave–wave interactions)

1 Introduction

Kinetic sound waves (KSWs) are an extension of plasma sound waves (or ion-acoustic waves) in the range of short (kinetic) perpendicular wavelengths $\lambda_\perp$ comparable to the ion gyroradius $\rho_i = V_{Ti}/\Omega_i$, $\lambda_\perp \sim \rho_i$. The wavelength parallel to the background magnetic field, λ_z, may remain in the magnetohydrodynamic (MHD) range. The finite gyroradius effects make KSWs far more interesting than their classic MHD counterparts. Because of the KSW dispersion modification at small perpendicular wavelengths, these waves become a decay-type mode in the frequency range below the ion cyclotron frequency (Hasegawa, 1976). Moreover, new channels for the KSW nonlinear coupling with other wave modes show up (Hasegawa and Chen, 1976; Brodin et al., 2006; Zhao et al., 2014). The varying phase velocity of KSWs opens more possibilities for Cherenkov-resonant wave–particle interactions that are not available for classic ion-sound waves. Also, similarly to low-frequency kinetic Alfvén waves (Voitenko and Goossens, 2005), KSWs can accelerate the ions nonadiabatically.

In situ and remote observations show that the sound waves (SWs) are a widespread phenomenon in the solar corona, solar wind, and Earth's magnetospheric and ionospheric plasma. For instance, the presence of significant levels of electrostatic activity in the solar wind, identified as ion-acoustic waves, has been confirmed by spacecraft observations (see review by Briand, 2009, and references therein). Spacecraft-frame frequencies of these waves are strongly Doppler-shifted by the solar wind, and their real plasma-frame frequencies can be significantly lower. The energy sources may be the electron heat flux or ion beams often observed in the solar wind.

Identification of widespread slow (acoustic) modes in different regions of the solar corona have revived interest in their application to coronal seismology (see recent papers by Ofman et al., 2012; Krishna Prasad et al., 2014, and references therein). Observed dissipation of these modes is difficult to explain by linear damping mechanisms (Krishna Prasad et al., 2014) and nonlinear theory is required. In the MHD low-frequency range, the slow-mode waves are

Published by Copernicus Publications on behalf of the European Geosciences Union.

almost electrostatic in low-β plasmas, like solar corona. High-frequency electrostatic SWs have been also involved in the modelling of type III radio bursts that trace the flare-accelerated electron beams in the solar corona and solar wind (see Thejappa et al., 2013, and references therein).

There has also been much interest in naturally occurring (as opposed to artificially stimulated) enhanced ion-acoustic spectra detected by incoherent scatter radars (ISRs) in the auroral zone and cusp/cleft region (see Sedgemore-Schulthess and St.-Maurice, 2001, for a review). They are easily distinguishable from the usual thermal back-scattering because of the strong enhancement of one or both ion-acoustic shoulders of the reflected radio signal. These two shoulders correspond to the ion-acoustic waves travelling away and towards the radar. The theoretical explanation of these naturally enhanced ion-acoustic lines is still a matter of debate.

As most space plasmas are non-uniform, KSWs can be created by the phase mixing of classic SWs, like in solar coronal loops (Voitenko et al., 2005). KSWs can also be generated linearly by shear plasma flows (Siversky et al., 2005) and nonlinearly by Alfvén waves (Zhao et al., 2014). In the present paper we study nonlinear interactions and decay instabilities of KSWs. One such instability has been considered previously in the framework of kinetic theory (Hasegawa, 1976). Here we use the electrostatic two-fluid plasma model that provides a good approximation for low-frequency KSWs. Our analytical results and conclusions differ in several respects from the results obtained by Hasegawa (1976) (see the Sects. 6 and 7 for the details). We apply our theoretical results to the conditions typical for the solar wind and topside Earth's ionosphere and conclude that the nonlinear spectral transport induced by the KSWs three-wave interactions can be faster than the wave damping in the solar wind and in the ionospheric F region. These results improve our understanding of nonlinear wave–wave interactions and spectral transport in solar and space plasmas.

2 Model

We consider a homogeneous hydrogen plasma in the ambient magnetic field directed along z axis in the Cartesian coordinate system. We are interested in the three-wave nonlinear interaction of electrostatic kinetic sound waves, particularly in the parametric decay KSW $\rightarrow$ KSW + KSW. To study this interaction, we use the nonlinear two-fluid magnetohydrodynamics in the electrostatic limit for perturbations. Our low-frequency KSWs are in fact the collisionless electrostatic counterparts of oblique MHD slow-mode waves, and hence our results are applicable only in low-β plasmas where the magnetic field is perturbed only slightly by these modes. The basic set of governing equations is

$$\nabla \cdot \boldsymbol{E} = 4\pi Q, \tag{1}$$

$$\frac{\partial \boldsymbol{V}_\alpha}{\partial t} + (\boldsymbol{V}_\alpha \nabla)\,\boldsymbol{V}_\alpha = \frac{q_\alpha}{m_\alpha}\left(\boldsymbol{E} + \frac{1}{c}\boldsymbol{V}_\alpha \times \boldsymbol{B}_0\right) - \frac{T_\alpha}{m_\alpha n_\alpha}\nabla n_\alpha, \tag{2}$$

$$\frac{\partial n_\alpha}{\partial t} = -\nabla \cdot (n_\alpha \boldsymbol{V}_\alpha), \tag{3}$$

where $Q = \sum_\alpha q_\alpha n_\alpha$ is the charge density and subscript $\alpha = e,\, i$ stands for the electron and ion species, respectively.

The total number density, velocity, electric field, and magnetic field are presented as

$$n_\alpha = n_0 + n_{\mathrm{p}} + n_1 + n_2,$$
$$\boldsymbol{V}_\alpha = \boldsymbol{V}_{\mathrm{p}} + \boldsymbol{V}_1 + \boldsymbol{V}_2,$$
$$\boldsymbol{E} = \boldsymbol{E}_{\mathrm{p}} + \boldsymbol{E}_1 + \boldsymbol{E}_2,$$
$$\boldsymbol{B} = B_0 \boldsymbol{e}_z,$$

where n_0 is the mean plasma density and $B_0\boldsymbol{e}_z$ is the ambient magnetic field. The subscript p indicates perturbations in the original (pump) wave, whereas the subscripts 1 and 2 indicate perturbations in two product waves.

We would like to note that, strictly speaking, kinetic ion sound waves and their nonlinear interaction can be rigorously described in the framework of kinetic theory. Instead, we use here the two-fluid MHD plasma model, as it gives a far more simple description and is still sufficiently accurate for the low-frequency waves we study.

3 Nonlinear dispersion relation for KSWs

In this section the nonlinear dispersion relation for kinetic sound waves is derived. In the electrostatic approximation the electric field of the sound wave can be presented as $\boldsymbol{E} = -\nabla\phi$, where ϕ is the wave electric potential. For low-frequency KSWs, the plasma approximation (quasineutrality condition) holds:

$$n_i = n_e. \tag{4}$$

This condition will be used in the derivations instead of the Poisson equation. Eliminating velocities by means of Eq. (2) we obtain from Eq. (3) the following ion density perturbation:

$$\frac{n_i}{n_0} = \frac{e}{m_i}\left(1 - \frac{V_{Ti}^2}{\omega^2}k_z^2 + \frac{V_{Ti}^2}{\Omega_i^2}k_\perp^2\right)^{-1} \times \left[\frac{k_z^2}{\omega^2}\left(1 - \frac{\omega^2}{k_z^2 V_s^2}\frac{V_s^2}{\Omega_i^2}k_\perp^2\right)\phi - N_i\right], \tag{5}$$

with the nonlinear part

$$N_i = -\frac{1}{\omega\Omega_i}\boldsymbol{b}_0\left[\boldsymbol{k}_\perp \times \boldsymbol{F}_{i\perp}\right] + \frac{i}{\Omega_i^2}k_\perp F_{i\perp} - \frac{i}{\omega^2}k_z F_{iz} - \frac{m_i}{en_0}\frac{\boldsymbol{k}}{\omega}\left(n_i \boldsymbol{V}_i\right)_{Nl},$$

where $\boldsymbol{F}_\alpha = -\frac{m_\alpha}{q_\alpha}\left(\boldsymbol{V}_\alpha \nabla\right)\boldsymbol{V}_\alpha$ and we assume harmonic plane waves $\sim \exp\left(-i\omega t + i\boldsymbol{k}\cdot\boldsymbol{r}\right)$. The cross $\times$ and dot $\cdot$ between vectors denote the vector and scalar products, respectively.

In the ion-sound waves the electron number density follows the Boltzmann distribution $n_e/n_0 = e\phi/T_e$. Then using the quasineutrality conditions (Eq. 4) we obtain the nonlinear dispersion relation for the amplitude Φ of the KSW electric potential:

$$\left(\omega^2 - \frac{k_z^2 V_T^2}{1+\mu}\right)\Phi = -\frac{\omega^2}{\mu+1}V_s^2 N_i. \tag{6}$$

Here $\mu = \left(V_T^2 k_\perp^2\right)/\Omega_i^2$, $V_T^2 = \left(T_e + T_i\right)/m_i$ and $V_s^2 = T_e/m_i$.

4 Resonant conditions

In the nonlinear coupling of KSWs, the waves must satisfy the resonant conditions $\omega_\mathrm{p} = \omega_1 + \omega_2$, $\boldsymbol{k}_\mathrm{p} = \mathbf{k}_1 + \boldsymbol{k}_2$. These conditions impose restrictions on the parameters of the interacting waves. For the analysis of the resonance conditions it is convenient to introduce the KSW dispersion function K,

$$K = K(\mu) = \frac{1}{\sqrt{1+\mu}},$$

and to present the KSW dispersion relation as $\omega = k_z V_T K$. From the frequency matching condition and z component of the wave-vector matching condition, we obtain $k_{1z}\left(s_1 K_\mathrm{p} - K_1\right) = k_{2z}\left(K_2 - s_2 K_\mathrm{p}\right)$, where $s_{1,2}$ denote the propagation directions of the product waves, such that $s_1 = s_2 = 1$ correspond to the co-propagating product KSWs and $s_1 = -s_2 = 1$ correspond to the counter-propagating product KSWs. It is assumed that the pump wave propagates in the direction of the background magnetic field.

The restricting condition directly follows from the above equations:

$$\left(s_1 K_\mathrm{p} - K_1\right)\left(K_2 - s_2 K_\mathrm{p}\right) > 0. \tag{7}$$

This condition arranges perpendicular wavenumbers in the following order: $K_2 > K_\mathrm{p} > K_1$ (or $K_1 > K_\mathrm{p} > K_2$) for the forward decay, and $K_\mathrm{p} > K_1$ for the reverse decay. This ordering can be rewritten in terms of μ: $\mu_1 > \mu_\mathrm{p} > \mu_2$ (or $\mu_2 > \mu_\mathrm{p} > \mu_1$) for the forward decay, and $\mu_1 > \mu_\mathrm{p}$ for the reverse decay.

5 Growth rate of the KSW decay

Using the linear responses due to the pump wave and the secondary KSWs, and retaining the dominant terms in the approximation $\omega \ll \Omega_i$, we obtain the nonlinearly coupled equations for the amplitudes of product KSWs. Thus, for the kinetic sound wave 1 we obtain the equation

$$\varepsilon_1 \Phi_1 = N_1 \Phi_\mathrm{p} \Phi_2^*, \tag{8}$$

where coefficients ε_1 and N_1 are

$$\varepsilon_1 = \omega_1^2 - k_{1z}^2 V_T^2 K_1^2,$$

$$N_1 = \omega_1 \Omega_i K_1^2 \left(\frac{e}{T_e}\right)\frac{V_T^2}{\Omega_i^2} i\boldsymbol{b}_0 \cdot \left[\boldsymbol{k}_{1\perp} \times \boldsymbol{k}_{2\perp}\right] \times \left[-\frac{V_T^2}{\omega_1 \omega_\mathrm{p}}\left[\frac{\omega_\mathrm{p}}{\omega_2}\left(\boldsymbol{k}_{1z}\cdot\boldsymbol{k}_{2z}\right) - \left(\boldsymbol{k}_{1z}\cdot\boldsymbol{k}_{\mathrm{p}z}\right)\right] + \frac{V_T^2}{\Omega_i^2}\left[\left(\boldsymbol{k}_{1\perp}\cdot\boldsymbol{k}_{2\perp}\right) + \left(\boldsymbol{k}_{1\perp}\cdot\boldsymbol{k}_{\mathrm{p}\perp}\right)\right] + \frac{m_e}{m_i}\left(K_\mathrm{p}^2 - K_2^2\right)\right].$$

The nonlinear equation for the second product KSW is the same as Eq. (8) but with exchanged subscripts 1 and 2. Splitting the frequency into real and imaginary parts, $\omega = \omega_{1,2} + i\gamma$, and combining Eq. (8) with the complex conjugate equation for the second product KSW, we arrive to the following nonlinear dispersion equation for the coupled KSWs:

$$\varepsilon_1 \varepsilon_2^* = N_1 N_2^* \left|\Phi_\mathrm{p}\right|^2.$$

For $\gamma \ll \omega_1, \omega_2$ we find the instability growth rate as

$$\gamma_\mathrm{NL}^2 = \frac{1}{4}\left|\frac{e}{T_e}\Phi_\mathrm{p}\right|^2 \frac{K_1 K_2}{K_\mathrm{p}^2}\Omega_i^2 \left[\frac{V_T^2}{\Omega_i^2}\boldsymbol{b}_0 \cdot \left(\boldsymbol{k}_{1\perp} \times \boldsymbol{k}_{2\perp}\right)\right]^2 \times \left(\frac{1}{K_\mathrm{p}} + \frac{s_1}{K_1} + \frac{s_2}{K_2}\right)^2 \left(K_2 - s_2 K_\mathrm{p}\right)\left(s_1 K_\mathrm{p} - K_1\right). \tag{9}$$

In the above expression we retain the dominant terms that occur in the parallel nonlinear force $\boldsymbol{k}_z \cdot \boldsymbol{F}_{iz}$ and perpendicular nonlinear force $\boldsymbol{b}_0 \cdot \left[\boldsymbol{k}_\perp \times \boldsymbol{F}_{i\perp}\right]$ and use the resonance conditions.

From the expression (9) we see that the growth rate γ is always real for the resonant waves, for which the ordering condition $\left(s_1 K_\mathrm{p} - K_1\right)\left(K_2 - s_2 K_\mathrm{p}\right) > 0$ holds. It is also seen that the growth rate is independent of k_z, which suggests a reduced rate of spectrum transport in the parallel direction.

6 Analysis of the forward and backward KSW decays

Here we analyse characteristics of KSW decays in more detail. To this end, we present the general expression of the normalized growth rate $\overline{\gamma}_\mathrm{NL}$ as a function of the normalized

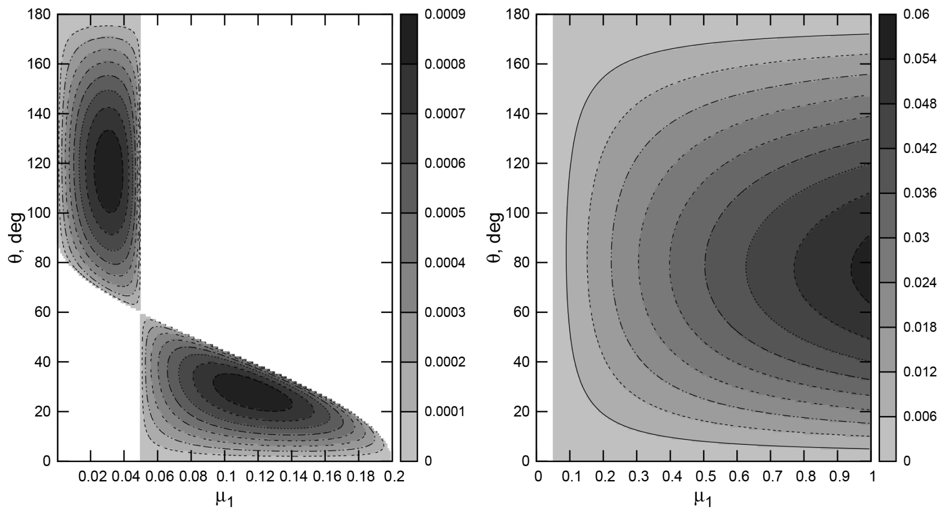

Figure 1. The normalized growth rate $\gamma / \left(\Omega_i \left|e\Phi_{\mathrm{p}}/T_e\right|\right)$ as a function of μ_1 and θ for small perpendicular wavenumber of the pump wave $\mu_{\mathrm{p}} = 0.05$. The left panel shows the forward decay and the right panel shows the reverse decay.

perpendicular wavenumber squared μ_1 and angle θ between $\boldsymbol{k}_{1\perp}$ and $\boldsymbol{k}_{\mathrm{p}\perp}$:

$$\overline{\gamma}_{\mathrm{NL}} = \frac{\gamma}{\left|\frac{e}{T_e}\Phi_{\mathrm{p}}\right|\Omega_i} = \frac{1}{2}\sqrt{\mu_1}\sqrt{\mu_{\mathrm{p}}}\left|\sin\theta\right| \times \left(\frac{1}{K_{\mathrm{p}}} + \frac{s_1}{K_1} + \frac{s_2}{K_2}\right) \left[\left(K_2 - s_2 K_{\mathrm{p}}\right)\left(s_1 K_{\mathrm{p}} - K_1\right)\frac{K_1 K_2}{K_{\mathrm{p}}^2}\right]^{1/2}, \tag{10}$$

where $\mu_2 = \mu_1 + \mu_{\mathrm{p}} - 2\sqrt{\mu_1\mu_{\mathrm{p}}}\cos\theta$.

The dependence of the normalized decay rate $\overline{\gamma}_{\mathrm{NL}}$ on the wave parameters μ_1 and θ is shown in Fig. 1. The left panel shows the growth rate for the forward decay ($s_1 = s_2 = 1$) and the right panel illustrates the reverse decay ($s_1 = -s_2 = 1$). In Fig. 1 we assume $\mu_{\mathrm{p}} = 0.05$ for the pump wave. We see that for forward decay there are two unstable regions in the $\mu_1 - \theta$ plane with the corresponding maximums at $\mu_1 \approx 0.6\mu_{\mathrm{p}}$; $\theta \approx 117°$, and at $\mu_1 \approx 2.3\mu_{\mathrm{p}}$; $\theta \approx 28°$. This behaviour can be understood from the restricting conditions $\mu_2 > \mu_{\mathrm{p}} > \mu_1$ (or $\mu_1 > \mu_{\mathrm{p}} > \mu_2$) for the forward decay. In the case of reverse decay we have only one unstable region ($\mu_1 > \mu_{\mathrm{p}}$) extended towards a large μ_1, where the growth rate gradually increases. This increase is not bounded in the two-fluid MHD model. But kinetic theory places an upper limit for the ion-acoustic waves in a Maxwellian plasma at μ_1 equal to about 4, depending on the ion to electron temperature ratio T_e/T_i. The peak value of the growth rate is distinctly larger for the reverse decay than for the forward decay.

We considered as well the higher value of the perpendicular wavenumber of the pump wave, i.e. $\mu_{\mathrm{p}} = 0.5$ and put the results in Fig. 2. Figure 2 shows that the peak values of the growth rate are larger (approximately in one order of magnitude) than that for $\mu_{\mathrm{p}} = 0.05$. It is seen that for the reverse decay the maximum of the growth rate shifts to the lower values of the angle θ.

Importantly, from Figs. 1 and 2 we see that the forward decay is local in $k_\perp$-space because all perpendicular wavenumbers in this decay are similar, $\mu_1 \sim \mu_2 \sim \mu_{\mathrm{p}}$. On the contrary, the reverse decay is nonlocal: product waves possess much larger perpendicular wavenumbers than the original pump wave, $\mu_1 \sim \mu_2 \gg \mu_{\mathrm{p}}$. As the reverse decay is in general significantly faster than the forward decay, the spectral transport induced by the three-wave KSW interactions is mostly nonlocal.

7 Application and discussion

The spectral transport induced by the nonlinear interaction among kinetic sound waves can be used for the explanation of wave phenomena in many solar and space plasmas. We consider here several possible examples.

First we analyse the nonlinear interaction of KSWs in the solar wind. The presence of a significant level of electrostatic activity identified as ion-acoustic waves has been recorded in the solar wind since the 1970s by the Helios and Voyager spacecrafts (Gurnett and Anderson, 1977; Gurnett and Frank, 1978; Gurnett et al., 1979). These waves were believed to propagate in the ion-acoustic mode, which is Doppler-shifted upward in frequency by the solar wind motion. The intensity of the waves varies between 1 to $10\,\mu\mathrm{V\,m^{-1}}$ in quiet periods of solar activity, but may reach a few tens of $\mu\mathrm{V\,m^{-1}}$ during more active periods. Using obtained analytical expressions for the KSW collisionless damping (Zhao et al., 2014) and nonlinear pumping rate, let us estimate the threshold amplitude for the decay using the following parameters

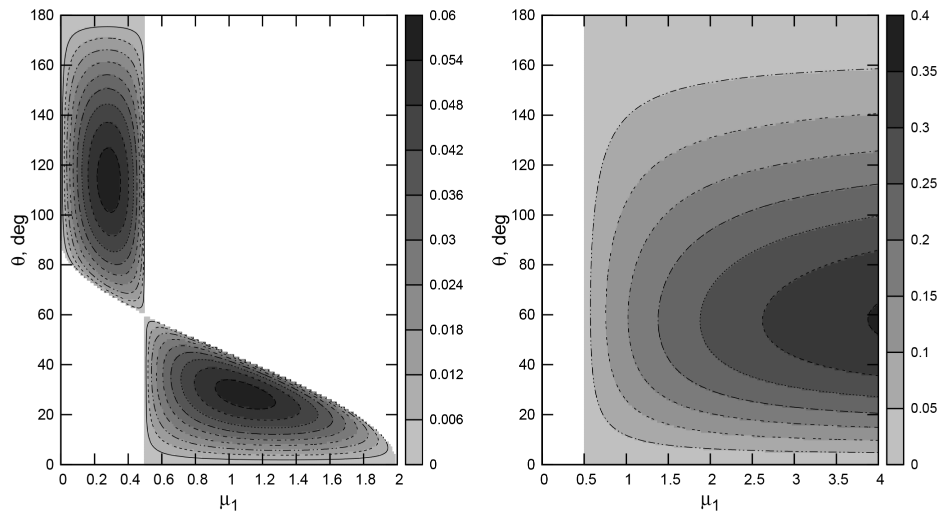

Figure 2. The same as in Fig. 1 but for $\mu_\mathrm{p} = 0.5$.

at 0.5 AU: $T_e = 1.5 \times 10^5$ K; $n_e = 1.2\,\mathrm{cm}^{-3}$; $B_0 = 5.3$ nT or $= 5.3 \times 10^{-5}$ G. With such plasma parameters $V_s = 3.5 \times 10^6\,\mathrm{cm\,s^{-1}}$, $\omega_{\mathrm{p}i}/\Omega_i \sim 3 \times 10^3$.

The nonlinear growth of the product waves may be balanced by their collisionless dissipation. Similarly to the parallel-propagating SWs, dissipation of oblique KSWs in weakly collisional plasmas is dominated by the Landau damping. The Landau damping occurs on both electrons and ions, with the relative importance depending on plasma parameters. As we consider plasmas with $T_e/T_i \sim 2$ the Landau damping on ions should be taken into account. The collisionless dissipation of kinetic ion-sound waves has been investigated by Zhao et al. (2014):

$$\gamma_{L\alpha} = \omega_\alpha g_\alpha, \qquad (11)$$

where $\alpha = 1, 2$ stands for two product KSWs, and coefficient

$$g_\alpha(\mu_i) = 0.14 - 0.61\left[\left(1 + \frac{T_i}{T_e}\right)\frac{0.42 + 0.58\mu_i}{0.42 + 0.038\mu_i} - 1\right]^{1/2} + 0.05\left[\left(1 + \frac{T_i}{T_e}\right)\frac{0.42 + 0.58\mu_i}{0.42 + 0.038\mu_i} - 1\right].$$

depends only on the normalized perpendicular wavenumber $\mu_i = \rho_i k_\perp$. Note the difference in our definition of μ_i ($\mu_i = \rho_i^2 k_\perp^2$) with that in Zhao et al. (2014).

The threshold amplitude for the pump wave to excite waves 1 and 2 can be obtained from the condition, $\gamma_{\mathrm{NL}}^2 = \gamma_{\mathrm{L1}}\gamma_{\mathrm{L2}}$, where γ_{NL} is the nonlinear pumping rate and $\gamma_{\mathrm{L1,2}}$ are the damping rates of product KSWs. Using above expressions for γ_{L1} and γ_{L2}, we obtain the threshold energy of the pump wave:

$$\left.\frac{W^s(k)}{n_e T_e}\right|_{\mathrm{thr}} = \frac{g_1(\mu_1)\, g_2(\mu_2)}{\overline{\gamma}_{\mathrm{NL}}^2}\frac{\omega_1\omega_2}{\Omega_i^2}\left(k_{\mathrm{pz}}\lambda_{\mathrm{De}}\right)^2. \qquad (12)$$

In Fig. 3a we plot the threshold amplitude of the pump wave as function of the pump wave frequency. For the forward decay the maximum $\overline{\gamma}_{\mathrm{NL}} \simeq 0.0009$ is attained at $\mu_1 \simeq 0.1$ and $\theta \simeq 28°$ (we have chosen here $\mu_1 > \mu_\mathrm{p} > \mu_2$). For the reverse case $\overline{\gamma}_{\mathrm{NL}} \simeq 0.056$ is attained at $\mu_1 \simeq 1$ and $\theta \simeq 77°$. In this figure $\mu_\mathrm{p} = 0.05$ and $T_e/T_i = 2$. It is seen that the threshold amplitude of the decay instability is very low for both decays. Note that for higher values of μ_p (say for $\mu_\mathrm{p} = 0.5$) we get even lower threshold amplitudes.

Here we consider decay instabilities of low-frequency kinetic sound waves with $\omega \ll \Omega_i$, which seems to lie below frequencies of the ion-sound turbulence observed by Gurnett and others. However, because of the limited resolution and other issues, the available solar wind observations (Voyager, Ulysses, Wind) cannot measure intensity of the ion-acoustic waves in the whole frequency/wavenumber domain (Melrose, 1982; Lacombe et al., 2002). Therefore the spectrum of non-thermal ion-sound waves may extend to lower frequencies, where our results are valid and indicate a strong decay instability. In future, we are going to consider the KSWs decays at higher frequencies, $\omega \gtrsim \Omega_i$ and $\omega \gg \Omega_i$. In most space plasmas, in particular in the solar wind, where the electrostatic turbulence has been observed, the ion plasma frequency is larger than the ion cyclotron frequency, $\omega_{\mathrm{p}i} > \Omega_i$, in which case the frequency domains $\omega \gtrsim \Omega_i$ and $\omega \gg \Omega_i$ seem to be relevant.

On the other hand, the low-frequency approximation that we used is directly applicable to the slow-mode waves observed in the solar corona (Krishna Prasad et al., 2014, and references therein) and solar wind (Howes et al., 2012, and references therein). The short dissipation distance of the coronal slow modes (Krishna Prasad et al., 2014) may result from their nonlinear decay into small-scale waves. The actual dissipation of the wave energy occurs at small scales and is of collisional nature in the solar coronal condi-

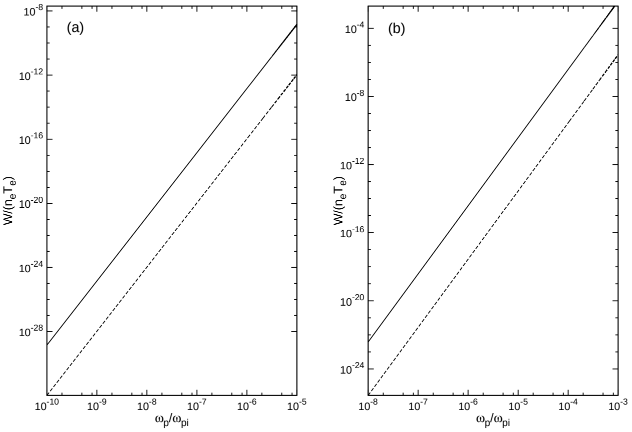

Figure 3. The dependence of threshold amplitude of pump wave on the frequency of pump wave for the maximum value of growth rate $\overline{\gamma}_{\rm NL} \simeq 0.0009$ for forward decay as well as for $\overline{\gamma}_{\rm NL} \simeq 0.056$ for reverse decay. Here we consider the parameters of solar wind plasma **(a)** as well as the plasma parameters of F region of Earth's ionosphere **(b)**. The solid line denotes the forward decay, and the dashed line denotes the reverse decay.

tions (Voitenko et al., 2005). In the solar wind turbulence the oblique slow-mode waves define the observed spectrum of compressible fluctuations (Howes et al., 2012). The possible contribution of nonlinear interactions among KSWs, studied in this paper, as compared to the interactions between KSWs and kinetic Alfvén waves (Zhao et al., 2014), is subject for future investigations.

The nonlinear interactions studied in our paper can also play a role in the topside Earth's ionosphere. The Naturally Enhanced Ion Acoustic Lines (NEIALs) are often observed at high latitudes in the incoherent scatter radar data. NEIALs appear as ion-acoustic fluctuations enhanced by two or three orders above the thermal level. The strength of one or both of the up- and down-shifted ion lines is increased (see Sedgemore-Schulthess and St.-Maurice, 2001, and references therein). Several theories have emerged in order to explain the source of NEIALs, namely the electron–ion and ion–ion two-stream instabilities as well as nonlinear wave–wave interactions (via Langmuir decay). The enhanced ion-acoustic fluctuations due to parametric decay of Langmuir waves remains the most promising, at least for explaining some observed features (see Kontar and Pécseli, 2005, and references therein).

A feasible explanation for two simultaneously observed spectral lines is provided by the nonlinear KSW interactions. If the plasma instabilities generate the ion-sound waves propagating in one direction, the reverse decay of these waves will generate the waves propagating in the opposite direction. As it is seen from Fig. 3b, the threshold amplitude for this decay is very low in the F region of Earth's ionosphere, where $T_e = 3100\,{\rm K}$; $T_i = 1400\,{\rm K}$; $n_e = 2\times10^5\,{\rm cm}^{-3}$; $B_0 = 0.5\,{\rm G}$ ($\omega_{\rm pi}/\Omega_i = 490$, $T_e/T_i = 2$). Here we would like to note the following. If the perpendicular wavenumbers of the waves is larger than their parallel wavenumbers, then the wavelengths of the reflected radio emission cannot be linked to the frequencies of ion-sound waves (parallel wavenumbers). In this case the KSW frequencies can be still in the low-frequency range and the low-frequency approximation used in our derivation can be still applicable. Otherwise higher KSW frequencies have to be accounted for (this work is in progress).

The nonlinear interaction of low-frequency kinetic ion-sound waves, with $\omega \ll \Omega_i$, has been considered by Hasegawa (1976) in the framework of kinetic theory. We would like to stress several differences between our result and results by Hasegawa (1976). According to Hasegawa (1976), the growth rate is determined by the parallel nonlinear force $\boldsymbol{k}_z \cdot \boldsymbol{F}_{iz}$ and only the reverse decay occurs. In the present paper we demonstrate that (i) the nonlinear terms $\sim \boldsymbol{k}_z \cdot \boldsymbol{F}_{iz}$ lead to the forward decay, not to the reverse one; (ii) the nonlinear terms due to the perpendicular nonlinear force $\boldsymbol{b}_0 \cdot [\boldsymbol{k}_\perp \times \boldsymbol{F}_{i\perp}]$ are as important as $\boldsymbol{k}_z \cdot \boldsymbol{F}_{iz}$ terms and must be taken into account. These terms make the forward decay 2–3 times faster and, most importantly, lead to a stronger reverse decay.

8 Conclusions

We studied the three-wave resonant interaction among kinetic sound waves. The nonlinear coupling equation describing both linear and nonlinear properties of KSWs is derived in the framework of a two-fluid plasma model. Because of the dispersive modification at small perpendicular wavelengths approaching the ion gyroradius, KSW become a decay-type mode. We derived the nonlinear decay rate of low-frequency KSWs with $\omega \ll \Omega_i$. The KSW Landau damping in the Maxwellian plasma is accounted for the range of temperature ratio $1/3 \lesssim T_e/T_i \lesssim 3$. Properties of the KSW decays can be summarized as follows:

1. There are two possible decay channels for KSWs: the forward decay into two co-propagating product KSWs ($k_{1z} > 0$, $k_{2z} > 0$) and the reverse decay into counter-propagating product KSWs ($k_{1z} > 0$, $k_{2z} < 0$).

2. Contrary to Hasegawa (1976), we found that the nonlinear terms $\sim \boldsymbol{k}_z \cdot \boldsymbol{F}_{iz}$ lead to the forward decay.

3. By accounting for the nonlinear terms $\sim \boldsymbol{b}_0 \cdot [\boldsymbol{k}_\perp \times \boldsymbol{F}_{i\perp}]$, overlooked by Hasegawa (1976), we found a much stronger reverse decay.

4. Both decay channels depend on the perpendicular wavenumber of the pump wave. The reverse decay rate for $\mu_{\rm p} = 0.5$ is approximately one order of magnitude larger than for $\mu_{\rm p} = 0.05$. The reverse decay is stronger than the forward decay for all $\mu_{\rm p}$.

5. In the forward decay the perpendicular wavenumbers of product KSWs are similar to the pump wavenumber, $\mu_1 \sim \mu_2 \sim \mu_{\rm p}$, which indicates the decay locality in $k_\perp$-space. On the contrary, the reverse-decay product KSWs have much larger perpendicular wavenumbers, $\mu_1 \sim \mu_2 \gg \mu_{\rm p}$, which makes this decay nonlocal. Since the reverse decay is stronger than the forward one, the spectral transport induced by three-wave KSW interactions is nonlocal.

6. The estimated thresholds of the KSW decays are very low in the solar wind and in the topside ionospheric conditions, which suggests their importance in these regions. The same may concern KSWs and their nonlinear dynamics in the solar corona and in laboratory plasmas.

7. The nonlinear interaction rate does not depend on the parallel wavenumbers, which reflects the dominant role of the perpendicular nonlinear dynamics where the parallel scales evolve kinematically.

These properties make KSW's nonlinear dynamics interesting in the context of acoustic-like wave activity observed in the solar corona, solar wind, and terrestrial magnetosphere.

Acknowledgements. This research was supported by the Belgian Federal Science Policy Office (via Solar-Terrestrial Centre of Excellence project "Fundamental science" and via IAP Programme project P7/08 CHARM) and by the European Commission (via FP7 Program project 313038 STORM).

Topical Editor V. Fedun thanks two anonymous referees for their help in evaluating this paper.

References

Briand, C.: Plasma waves above the ion cyclotron frequency in the solar wind: a review on observations, Nonlin. Processes Geophys., 16, 319–329, doi:10.5194/npg-16-319-2009, 2009.

Brodin, G., Stenflo, L., and Shukla, P. K.: Nonlinear Interactions Between Kinetic Alfvén and Ion-Sound Waves, Solar Phys., 236, 285–291, doi:10.1007/s11207-006-0125-2, 2006.

Gurnett, D. A. and Anderson, R. R.: Plasma wave electric fields in the solar wind Initial results from HELIOS 1, J. Geophys. Res., 82, 632–650, doi:10.1029/JA082i004p00632, 1977.

Gurnett, D. A. and Frank, L. A.: Ion acoustic waves in the solar wind, J. Geophys. Res., 83, 58–74, doi:10.1029/JA083iA01p00058, 1978.

Gurnett, D. A., Marsch, E., Pilipp, W., Schwenn, R., and Rosenbauer, H.: Ion acoustic waves and related plasma observations in the solar wind, J. Geophys. Res., 84, 2029–2038, doi:10.1029/JA084iA05p02029, 1979.

Hasegawa, A.: Decay of ion acoustic wave in magnetized plasma, Phys. Lett., 57A, 143–144, doi:10.1016/0375-9601(76)90192-4, 1976.

Hasegawa, A. and Chen, L.: Parametric Decay of "Kinetic Alfvén wave" and its application to plasma hetaing, Phys. Rev. Lett., 36, 1362–1365, doi:10.1103/PhysRevLett.36.1362, 1976.

Howes, G. G., Bale, S. D., Klein, K. G., Chen, C. H. K., Salem, C. S., and TenBarge, J. M.: The Slow-mode Nature of Compressible Wave Power in Solar Wind Turbulence, Astrophys. J. Lett., 753, L19, doi:10.1088/2041-8205/753/1/L19, 2012.

Kontar, E. P. and Pécseli, H. L.: Nonlinear wave interactions as a model for naturally enhanced ion acoustic lines in the ionosphere, Geophys. Res. Lett., 32, L05110, doi:10.1029/2004GL022182, 2005.

Krishna Prasad, S., Banerjee, D., and Van Doorsselaere, T.: Frequency-dependent Damping in Propagating Slow Magneto-acoustic Waves, Astrophys. J., 789, 118, doi:10.1088/0004-637X/789/2/118, 2014.

Lacombe, C., Salem, C., Mangeney, A., Hubert, D., Perche, C., Bougeret, J.-L., Kellogg, P. J., and Bosqued, J.-M.: Evidence for the interplanetary electric potential? WIND observations of electrostatic fluctuations, Ann. Geophys., 20, 609–618, doi:10.5194/angeo-20-609-2002, 2002.

Melrose, D. B.: Fundamental emission for type III bursts in the interplanetary medium: the role of ion-sound turbulence, Solar Phys., 79, 173–185, doi:10.1007/BF00146981, 1982.

Ofman, L., Wang, T. J., and Davila, J. M.: Slow Magnetosonic Waves and Fast Flows in Active Region Loops, Astrophys. J., 754, 111, doi:10.1088/0004-637X/754/2/111, 2012.

Sedgemore-Schulthess, F. and St.-Maurice, J.-P.: Naturally enhanced ion-acoustic spectra and their interpretation, Surv. Geophys., 22, 55–92, doi:10.1023/A:1010691026863, 2001.

Thejappa, G., MacDowall, R. J., and Bergamo, M.: Evidence for four- and three-wave interactions in solar type III radio emissions, Ann. Geophys., 31, 1417–1428, doi:10.5194/angeo-31-1417-2013, 2013.

Voitenko, Y. and Goossens, M.: Nonlinear coupling of Alfvén waves with widely different cross-field wavelengths in space plasmas, J. Geophys. Res., 110, A10S01, doi:10.1029/2004JA010874, 2005.

Voitenko, Y., Andries, J., Copil, P. D., and Goossens, M.: Damping of phase-mixed slow magneto-acoustic waves: Real or apparent?, Astron. Astrophys., 437, L47–L50, doi:10.1051/0004-6361:200500134, 2005.

Siversky, T., Voitenko, Y., and Goossens, M.: Shear Flow Instabilities in Low-Beta Space Plasmas, Space Sci. Rev., 121, 343–351, doi:10.1007/s11214-006-7182-6, 2005.

Zhao, J. S., Voitenko, Y. M., Wu, D. J., and De Keyser, J.: Nonlinear Generation of Kinetic-Scale Waves by MHD Alfvén Waves and Nonlocal Spectral Transport in the Solar Wind, Astrophys. J., 785, 139, doi:10.1088/0004-637X/785/2/139, 2014.